Characteristics of microwave photonic signal generation using vertical-cavity surfaceemitting lasers with optical injection and feedback

Xu, Chenpeng; Chang, Da; Fan, Yuanlong; Ji, Songkun; Zhang, Zuxing; Lin, Hong; Spencer, Paul; Hong, Yanhua

Journal of the Optical Society of America B: Optical Physics

DOI:
https://doi.org/10.1364/JOSAB.389890

Published: 01/05/2020

Peer reviewed version

Characteristics of microwave photonic signal generation using vertical-cavity surface-emitting lasers with optical injection and feedback

CHENPENG XUE[1], DA CHANG[2], YUANLONG FAN[2, 3], SONGKUN JI[2, 4], ZUXING ZHANG[1], HONG LIN[5], PAUL S. SPENCER[2] AND YANHUA HONG[2,*]

[1] *The Advanced Photonics Technology Lab, College of Electronics and Optical Engineering & College of Microelectronics, Nanjing University of Posts and Telecommunications, Nanjing, 210023, China.*
[2] *The School of Computer Science and Electronic Engineering, Bangor University, Bangor LL57 1UT, U.K.*
[3] *Wireless & Optoelectronics Research & Innovation Centre, Faculty of Computing, Engineering & Science, University of South Wales, Wales, CF37 1DL, UK.*
[4] *Key Laboratory of the Ministry of Education for Optoelectronic Measurement Technology and Instrument, Beijing Information Science & Technology University, Beijing, 100192, China*
[5] *Department of Physics and Astronomy, Bates College, Lewiston, ME 04240, USA*
**y.hong@bangor.ac.uk*

Abstract: Characteristics of microwave photonic signal generation based on P1 dynamic in an optically injected vertical-cavity surface-emitting laser are studied systematically. The evolutions of the linewidth, power and second harmonic ratio of the generated microwave are investigated as a function of injection strength and frequency detuning. The effect of optical feedback on the linewidth and the phase noise of the generated microwave photonic signal is also studied in detail. With the help of optical feedback, the linewidth can be effectively reduced by increasing the feedback strength and feedback delay time. However, there is an optimal feedback delay time to minimize the phase noise.

1. Introduction

Microwave photonic signal generation technologies have gained considerable attention because of potential applications in broadband wireless access networks, sensor networks, radar, satellite communications, instrumentation, and so on. The technologies for generating microwave photonic signal can be categorized as direct modulation, optical heterodyne technique, external modulation, mode-locked semiconductor lasers, optoelectronic oscillator and the period one (P1) oscillation [1]-[6].

Semiconductor lasers with external optical injection can exhibit various dynamics states, for instance, stable locking, P1 oscillation, period-two oscillation, quasi-periodic oscillation and chaos fluctuation. Among them, the P1 dynamic occurs when stable locking is broken and the system starts to experience Hopf-bifurcations [7], in which two dominant frequencies are induced, one stems from the optical injection, while the other one is the red-shifted cavity frequency. Obviously, a microwave photonic signal can be generated by utilizing the beating of the two dominant frequencies in the P1 dynamic. Compared to other techniques, microwave photonic signal generation based on P1 oscillation has many advantages, such as a nearly single sideband (SSB) spectrum, low cost, all-optical components configuration, and widely tunable microwave frequency far from its relaxation resonance frequency [8], [9]. Microwave photonic signal generation based on P1 oscillation has mainly been investigated

in distributed feedback (DFB) lasers [4], [7], [9], [10]. There have also been some reports using quantum dot lasers [11]-[13].

Vertical-cavity surface-emitting lasers (VCSELs) have many desired features, such as circular beam profile, single-longitudinal mode operation, ease of fabrication, low power consumption and low-cost, therefore could be an excellent candidate for microwave photonic signal generation [14]. Quirce et al. predict that microwave photonic signal can be generated using a multi-mode VCSEL subject to two frequency orthogonal optical injection [15]. In 2015, 20 GHz microwave photonic signal was obtained using double-beam orthogonal optical injection in a single-transverse-mode VCSEL [16]. Lin et al. also experimentally achieved microwave photonic signal in a multimode VCSEL subject to orthogonal optical injection [17]. Our team has recently experimentally demonstrated tunable-frequency microwave photonic signal generation utilizing single-mode VCSEL's P1 oscillation [18].

Despite many advantages of microwave photonic signal generation based on P1 oscillation, it does not come without the disadvantages. The inherent phase noise in the nonlinear P1 oscillation due to the spontaneous emissions harms its applications. For instance, the phase noise can reduce the signal-to-noise ratio in communications [19]. The phase noise can also increase the linewidth of the generated microwave, which affects the performance in radio over fiber (RoF) applications and the maximum detection range in Doppler velocimeters [20], [21]. To solve this problem, many methods have been introduced, such as using double-locking with a microwave source [12], [22], [23], optoelectronic feedback [24], [25] and optical feedback [9], [26]-[28]. Among all of these schemes, optical feedback is a simple and low-cost method to reduce the phase noise and linewidth. The use of optical feedback to reduce phase noise and linewidth has been theoretically and experimentally proven in DFB lasers. Using double optical feedback to narrow the microwave photonic signal linewidth has also been experimentally demonstrated in a VCSEL [29]. In addition, fluctuations in the power and frequency of the injected laser lead to significant microwave frequency jitters, which seriously affects the applications of microwave photonic signal generated based on P1 oscillation. The scheme of optical modulation sideband injection locking has been proposed and experimentally demonstrated to stabilize the microwave photonic signal [30]. We also recently experimentally study the stabilization of microwave photonic signal generation based on P1 oscillation in a VCSEL with optical feedback [31].

However, to the best of our knowledge, the quantitative characterization of microwave photonic signal generation using the period-one oscillation of a VCSEL, including linewidth, phase noise, power and second harmonic ratio (SHR), has not been theoretically studied. In this work, the microwave photonic signal generation based on P1 oscillation of VCSEL with optical injection and feedback is systemically investigated. The paper is organized as follows. The theoretical model is described in Section 2, followed by the numerical simulation results in section 3. Finally, we summarize the results in section 4.

2. Theoretical Model

The dynamics of optically injected VCSEL with two optical feedbacks are fully described by the temporal evolution of the complex optical field and the charge carrier density. Here, the most common spin-flip model for VCSELs is adopted to simulate the complex electric field E, the total carrier density N, and the difference between the carrier densities with opposite spin values n [30]-[32], which are described as:

$$\frac{\partial E_x}{\partial t} = k(1+i\alpha)(NE_x - E_x + inE_y) - (\gamma_a + i\gamma_p)E_x + \eta_x E_{inj} e^{i2\pi(f_{inj}-f_0)t} + \xi_1 E_x(t-\tau_1)e^{-i2\pi f_0 \tau_1} + \xi_2 E_x(t-\tau_2)e^{-i2\pi f_0 \tau_2}$$

$$+\left(\sqrt{\frac{R_+}{2}}\vartheta_+(t)+\sqrt{\frac{R_-}{2}}\vartheta_-(t)\right) \tag{1}$$

$$\begin{aligned}\frac{\partial E_y}{\partial t} &= k(1+i\alpha)(NE_y - E_y - inE_x)\\ &+(\gamma_a+i\gamma_p)E_y+\eta_y E_{inj}e^{i2\pi(f_{inj}-f_0)t}\\ &+\xi_1 E_y(t-\tau_1)e^{-i2\pi f_0\tau_1}+\xi_2 E_y(t-\tau_2)e^{-i2\pi f_0\tau_2}\\ &-i\left(\sqrt{\frac{R_+}{2}}\vartheta_+(t)-\sqrt{\frac{R_-}{2}}\vartheta_-(t)\right)\end{aligned} \tag{2}$$

$$\begin{aligned}\frac{\partial N}{\partial t} &= -\gamma_e N(1+|E_x|^2+|E_y|^2)+\gamma_e\mu\\ &-i\gamma_e n(E_yE_x^*-E_xE_y^*)\end{aligned} \tag{3}$$

$$\begin{aligned}\frac{\partial n}{\partial t} &= -\gamma_s n-\gamma_e n(|E_x|^2+|E_y|^2)\\ &-i\gamma_e N(E_yE_x^*-E_xE_y^*)\end{aligned} \tag{4}$$

where the subscripts x and y stand for the X and Y polarizations of the VCSEL, respectively. α is the linewidth enhancement factor; γ_a is the linear dichroism; γ_p is the linear birefringence; γ_e is the decay rate of the total carrier population; k is the field decay rate; γ_s is the spin-flip rate; η_x and η_y are the injection strength into the X and Y polarization direction, respectively; E_{inj} is the injection field amplitude. $f_o = (f_x + f_y)/2$ is the center frequency of the free running VCSEL, where $2\pi f_x = 2\pi f_0 + \alpha\gamma_a - \gamma_p$ and $2\pi f_y = 2\pi f_0 + \gamma_p - \alpha\gamma_a$ are the frequency of the X and Y polarization components, respectively. f_{inj} is the injection frequency. The frequency detuning $\Delta f = f_{inj} - f_0$; ξ_1 and ξ_2 are the feedback strength of each feedback cavity; τ_1 and τ_2 are the feedback delay times of feedback loop 1 and 2, respectively; μ is the normalized bias current. Moreover, the spontaneous emission noise rates R_+ and R_- are also taken into account in our model, which are described as [32],

$$R_\pm = \beta_{SF}\gamma_e\left((N\pm n)+\frac{G_N N_t}{2k}\right) \tag{5}$$

where β_{SF} is the coefficient of spontaneous emission and G_N is the differential gain. As for the fluctuations of spontaneous emission, the complex Gaussian noise terms $\vartheta_-(t)$ and $\vartheta_+(t)$ have a mean of zero and variance of one and are given by

$$\left\langle \vartheta_i(t)\vartheta_j^*(t')\right\rangle = \delta_{ij}\delta(t-t') \tag{6}$$

In the simulation, only in-phase optical feedback is considered to simplify the investigation. For the sake of simplicity, the Gaussian noise terms are assumed to has finite variance, and the fourth order Runge-Kutta integration method is used to numerically solve equations (1)–(4), where a temporal resolution of Δt = 1ps is selected and the duration of the time series is 100 μs. The parameters listed in Table 1 are used in the simulation. These parameters are extracted from the experimental results [32]. With these typical parameters,

the VCSEL works in the Y-polarization. Parallel injection (η_x =0 ns^{-1} and η_y ≠0 ns^{-1}) is considered and η_y is labeled as η. It is worth mentioning that in order to simulate the linewidth observed in the experiment [31], a relatively large spontaneous emission coefficient is selected for the Gaussian noise terms.

Table 1. Summary of the parameters

Parameter names	Symbol	Value
Linewidth enhancement factor	α	2.8
Line dichroism	γ_a	5 ns^{-1}
Line birefringence	γ_p	16 ns^{-1}
Decay rate of the total carrier population	γ_e	2.08 ns^{-1}
Field decay rate	κ	33 ns^{-1}
Spin-flip rate	γ_s	2100 ns^{-1}
Injection filed amplitude	E_{inj}	1
Normalized bias current	μ	2
Coefficient of spontaneous emission	β_{SF}	1×10^{9}
The differential gain	G_N	$2.152\times10^{4}s^{-1}$
The transparent carrier number	N_t	9×10^{6}
Center frequency of the VCSEL	f_0	193.55THz

3. Microwave photonic signal generation

3.1 Optical injection only

The P1 oscillation in a VCSEL subject to optical injection is utilized for the microwave photonic signal generation. For the case of optical injection only, the characteristics of the generated microwave including the linewidth and frequency are mainly determined by the injection parameters (Δf, η). To gain an insight into the evolution of the characteristics of the microwave signal versus the injection parameters, the linewidth and frequency are examined firstly in this section. In this work, the linewidth is calculated by smoothing and a Lorenzian fitting. As shown in Fig.1, the color region corresponds to the P1 oscillation regime. The microwave frequency increases with an increase of the injection strength and the absolute frequency detuning. By properly setting the injection parameters, the generated microwave frequency can be much higher than the frequency shown in Fig. 1. In terms of the microwave linewidth, there is an evident linewidth narrowing region located in the area of small injection strength and small frequency detuning. Unfortunately, it only covers a small range of microwave frequency. The closer to Hopf-bifurcation, the wider the linewidth is, especially for case with strong injection strength. The other area in the P1 region holds a similar medium linewidth of about 5MHz. It is noted that the medium linewidth region covers a much wider range of the microwave frequency, which is different from that in DFB lasers [21]. It has also been reported that some specific operating points near this low linewidth region are less sensitive to perturbations [33]; however, this phenomenon is beyond the scope of this paper.

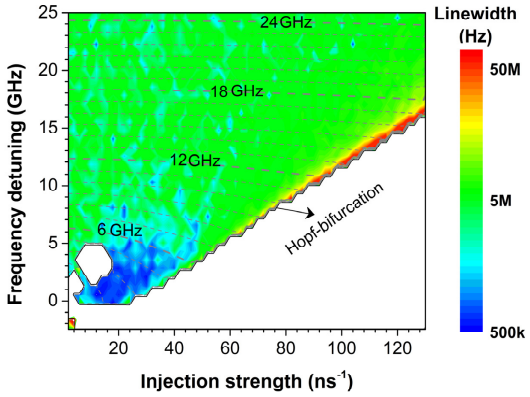

Fig. 1. Linewidth and microwave frequency (dash line) as a function of injection strength and frequency detuning.

The power of microwave is also a key parameter used to evaluate the generated microwave signal. The power of the microwave signal here is defined as the peak power at the fundamental frequency in the power spectum. Fig. 2 shows the microwave power as a function of the injection parameters. Similar to the linewidth, there is a region with relatively high power located at the small injection parameters area, which corresponds to a relatively low fundamental frequency. It is worth mentioning that there is a special range of injection parameters (the area is drawn by a black line), where relatively high microwave powers are obtained with a broad range of the microwave frequency. Outside this range, the power reduces gradually. In Fig. 1, there are some small regions in the weak injection strength areas where a relatively narrow linewidth can be achieved with a large frequency detuning, but the microwave power is low in these regions, as shown in Fig. 2.

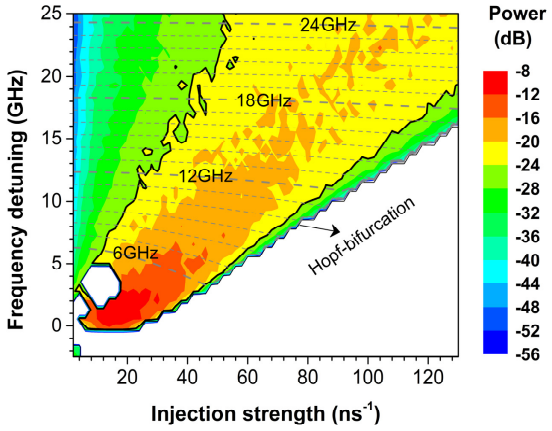

Fig. 2. Power and microwave frequency (dash line) as a function of injection strength and frequency detuning.

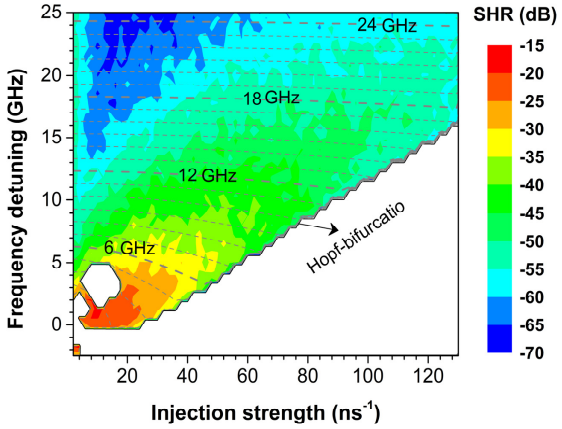

Fig. 3. SHR and microwave frequency (dash line) as a function of injection strength and frequency detuning.

Second harmonic ratio (SHR) as a function of the injection parameters is also studied. Here, the SHR is defined as the power ratio of the power at the second harmonic frequency to the power at the fundamental frequency. The results in Fig.3 illustrate that a high SHR region is located in a region of lower microwave frequency. With the increase of microwave frequency, the SHR drops. Moreover, there is also evidence of lower SHR located at the low power area indicated in Fig.2. To some extent, the higher SHR area coincides with the higher microwave power area. As the second harmonic is undesired in the single frequency microwave source, there is a trade-off between the higher microwave power and lower SHR.

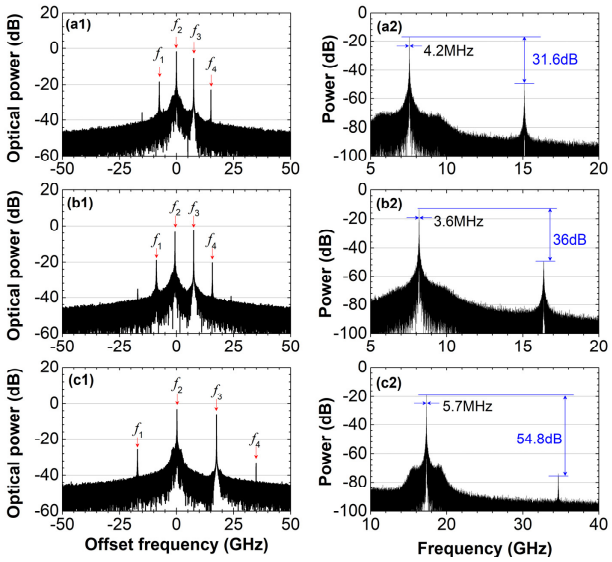

Fig. 4. Optical spectra (left column) and RF power spectra (right column) of the VCSEL with different injection parameters, (a) Δf =7.546 GHz, η=20 ns^{-1}, (b) Δf =7.546 GHz, η=40 ns^{-1}, (c) Δf =17.546 GHz, η=40 ns^{-1}.

In order to explain the evolutions of power and SHR, the optical and RF power spectra are studied. Fig. 4(a) shows the case with injection parameters of Δf =7.546 GHz and η=20 ns^{-1}. The largest four frequency components in the optical spectrum are named *f1* to *f4* from

the left to the right, as labeled in the figure. f_2 and f_3 are the red-shift cavity resonance frequency and injecting frequency from the master laser, respectively. The fundamental microwave frequency at 7.55 GHz with a linewidth of 4.2 MHz and a power of -17.3 dB shown in Fig. 4(a2) is mainly stemmed from the beating of the components at f_2 and f_3, and the second harmonic comes from the combined beating of the components at f_1 and f_3, and f_2 and f_4. When we increase the injection strength to 40 ns^{-1}, as shown in Fig. 4(b), the components corresponding to f_3 and f_4 increases, but the components related to f_1 and f_2 have a small reduction. As a result, the power of f_3 is close to that of f_2, and the microwave power is enhanced. It is reasonable to deduct that further increasing the injection strength, the power of f_3 would exceed the power of f_2 and the power of the microwave at the fundamental frequency drops. The SHR is dependent on the powers of the fundamental frequency and harmonic frequency and both powers vary with the injection parameters. In Fig. 4(b), there is a greater increase in the fundamental frequency power relative to that of the second harmonic, as a result, there is a slightly drop in SHR from -31.6 dB to -36 dB. In Fig. 3, the SHR at the lower injection strength is lower than that observed at the higher injection strength and this can be attributed to a reduction in the power of the second harmonic. In Fig. 4(b2), the fundamental microwave frequency is also shifted to 8.2 GHz and the linewidth reduces to 3.6 MHz. When the injection frequency detuning is increased to 15 GHz, as shown in Fig. 4(c), the powers of the four frequency components reduce, especially for the components of f_1 and f_4. Therefore, both the powers of the fundamental frequency and the second harmonic frequency are reduced and the SHR decreases to 54.8 dB. However, the fundamental microwave frequency increases to 17. 33 GHz and the linewidth is 5.7MHz.

3.2 P1-ocsillation with optical injection and feedback

Polarization reserved optical feedback is then added to narrow the linewidth of the microwave photonic signal in this study. In this section, the injection parameters are the same as those in Fig. 4(a). Fig. 5 shows the optical and power spectra of the VCSEL. The case of P1-oscilation with single feedback (ξ_1=ξ=1 ns^{-1}, ξ_2 =0 and τ_1 = τ =5ns) is shown in Fig. 5 (a). The linewidth is obviously reduced from 4.2 MHz without optical feedback to 39.6 kHz with optical feedback. Fig.5 (a2) also shows many side peaks which correspond to the external cavity modes' frequencies. To quantitatively estimate the sizes of the side-peaks, we define the side peak suppression coefficient as the power ratio between the fundamental frequency power and the maximum side-peak power. In Fig. 5(a2), the side peak suppression coefficient is ~ 36 dB. With double optical feedback, as shown in Fig. 5(b), the linewidth is 52.9 kHz, which is slightly larger than that with single feedback for this feedback strength, but the side peak suppression coefficient is increased to 48 dB. Similar phenomenon has been experimentally demonstrated in our previous work [31]. Moreover, except f_3, the power of the other three frequency components with optical feedback in Fig. 5(a1) and (b1) are also increased, which results in an increase of the fundamental microwave frequency power. It is worth mentioning that the microwave frequency is also changed with the optical feedback, which is similar to the report in [26]. But the frequency shift due to the optical feedback is much less than that in [26]. Using the same optical injection parameters used in Fig. 3(a), the microwave frequency shifts from 7.55 GHz to 7.565 GHz and 7.578 GHz when the feedback strengths are 0.07 ns^{-1} and 1.65 ns^{-1}, respectively.

Fig. 6 illustrates the linewidth reduction versus the feedback strength. As we expected, with the increasing of the feedback strength, the linewidth manifests a rapidly decrease in both the single and double feedback schemes. When the feedback strength is over 1.65 ns^{-1}, the linewidth exhibits an oscillating increase. This can be attributed to the VCSEL starting to move out of P1 dynamic to the other nonlinear dynamics regimes [as demonstrated by the insets of Figs. 6(a) and (b)]. It is noted that there is no evidence of a linewidth difference between the single and double feedback schemes when the total feedback strength is below 2 ns^{-1}.

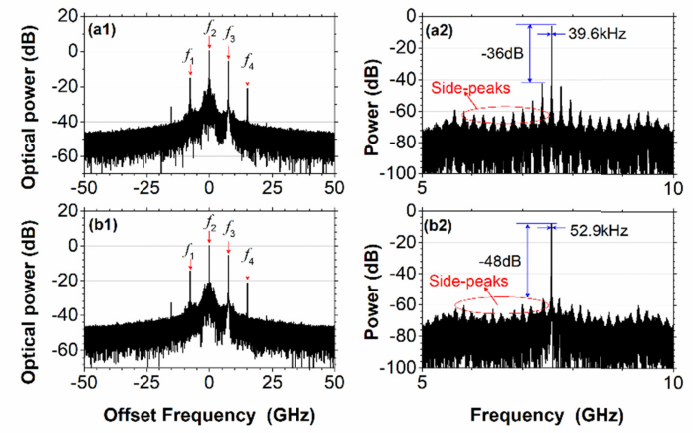

Fig.5 Optical spectra (left column) and RF power spectra (right column) of the VCSEL, (a) single feedback with ξ=1ns^{-1} and τ=5 ns, (b) double feedback with ξ_1= ξ_2 = 0.5 ns^{-1}, τ_1=5 ns and τ_2=6.7 ns.

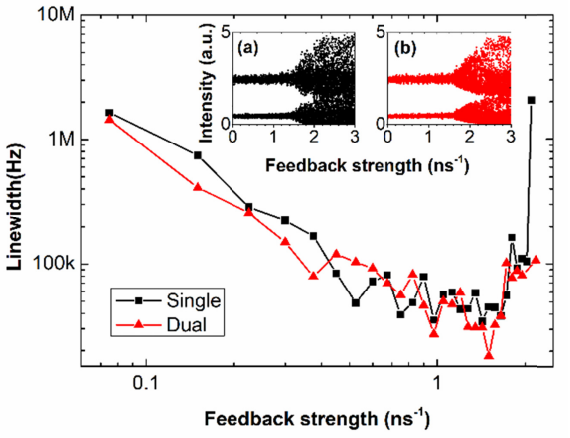

Fig. 6. Linewidth as a function of the total feedback strength, Δf =7.546 GHz, η=20 ns^{-1}, τ_1=5 ns and τ_2=6.7 ns. The feedback strengths in the two feedback loops for double feedback scheme are set equally. Insets (a) and (b) are bifurcation of the VCSEL with single and double feedback, respectively.

Fig. 7 presents the phase noise evolution with the variation of the feedback strength. The phase noise is calculated by integrating the averaged single sideband of the power spectrum centered at the fundamental frequency over an offset from 3 MHz to 1 GHz and normalizing to the microwave power [21]. The phase variance is proportional to the integrated mean square timing jitter of the P1 oscillation. In the linewidth reduction region, the phase noise drops with the increasing of feedback strength, until a minimum value is reached. Out of this region, the phase noise increases dramatically. This is because both the non-zero linewidth and side-peaks contribute to the phase noise. Compared with the case of dual feedback, the phase noise in the case of single feedback is relatively large, especially for strong feedback. This is due to the stronger side-peaks in the power spectra for single feedback. Effects of optical feedback on the microwave power and second harmonic ratio are also calculated and shown in the insets of Fig. 7. The results show that the microwave power and SHR increase slowly with increasing feedback strength, and then stabilize at the values of ~ -14 dB and ~ -32.5 dB, respectively, until the P1 is broken.

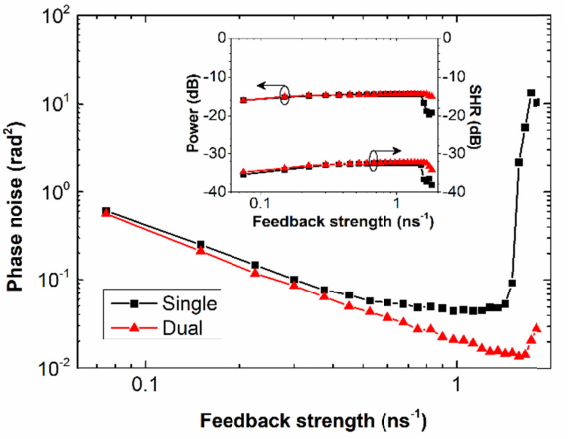

Fig. 7. Phase noise as a function of the total feedback strength. The injection and feedback parameters are the same as those used in Fig. 6. Insets are the power and SHR of the microwave signal as a function of the total feedback strength.

Fig. 8 shows the influence of the feedback delay time on the linewidth and phase noise of the generated microwave based on P1 oscillation with single feedback. The feedback strength is 0.1 ns^{-1} and the injection parameters are the same as those in Fig. 4(a). The result shows that the linewidth decreases monotonically with increasing feedback delay time. Thus, a longer external cavity is good for the linewidth reduction. However, the phase noise shows a different trend. With the increase of the feedback delay time, the phase noise first shows a drop, and then rises when the delay time is longer than 16 ns. This is because the density of the side-peaks increases with increasing feedback delay time. These results are similar to those in [21]. The abrupt changes of the microwave linewidth and phase noise in [26], [34] are not observed. The difference between the results in Fig. 8 and the results in [26],[34] is due to the different feedback round trip time. The feedback round trip times used in [26] and [34] are less than 1.2ns. Fig. 8 in [26] shows that the abrupt changes of the microwave linewidth and phase noise become less obvious when the feedback round trip time is more than 1ns.

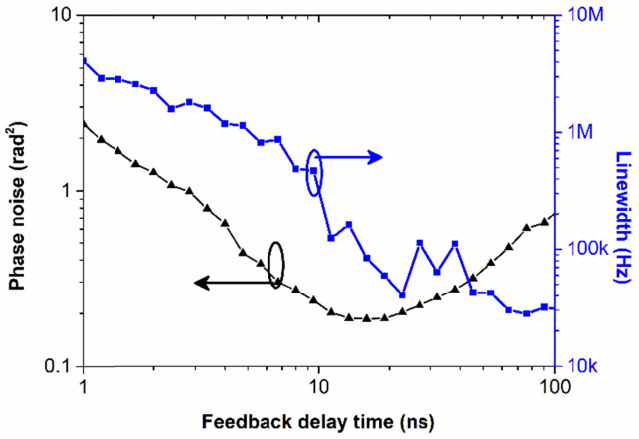

Fig. 8. Linewidth and phase noise as a function of the feedback delay time in single feedback loop, Δf=7.546 GHz, η=20 ns^{-1} ξ=0.1 ns^{-1}.

Compared with single feedback, double feedback has a more complex parameter set. The phase noise versus the feedback strength ratio between the two feedback loops is studied.

Fig. 9 shows the phase noise as a function of the feedback strength ratio with three different total feedback strengths (0.4 ns^{-1}, 0.8 ns^{-1} and 1.2 ns^{-1}). The results illustrate that the variation trends of the phase noise versus the feedback strength ratio with the different total feedback strength are similar. With an increase in the feedback strength ratio, the phase noise first decreases, reaches a minimum value at the ratio of ~1, and then rises again. This can be interpreted as the side-peaks suppression due to the competition of the external-cavity modes. Using similar feedback strength for the two feedback loops improves the side peaks suppression. In addition, Fig. 9 exhibits that the phase noise reduces with an increase of the total feedback strength. This can be attributed to the linewidth reduction associated with an increase of the feedback strength.

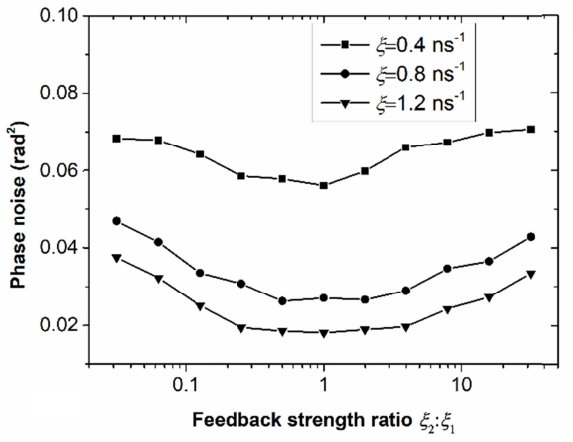

Fig. 9. Phase noise as a function of the feedback strength ratio between the two feedback loops, Δf=7.546 GHz, η=20 ns^{-1}, τ_1=5 ns and τ_2=6.7 ns.

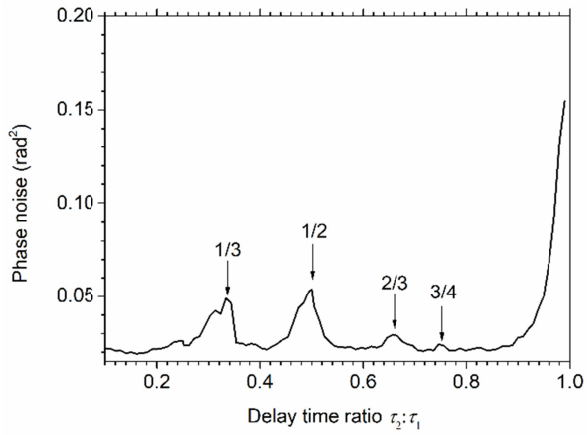

Fig.10. Phase noise as a function of the feedback delay time ratio between the two feedback loops. Δf=7.546 GHz, η=20 ns-1, $\xi_1 = \xi_2$ = 0.5 ns^{-1} and τ_1=20 ns.

Since dual feedback setup has two feedback delay times, the effect of feedback delay time on phase noise cannot be plotted in the format of Figure 8. Instead, the effect of feedback delay time ratio between the two feedback loops is investigated and the result is displayed in Fig. 10. In the study, the feedback strengths in the two feedback loops are set equally at 0.5ns^{-1}, the delay time of feedback loop 1 is fixed at 20 ns, whilst the delay time of feedback loop 2 is varied. The region with $\tau_2 > \tau_1$ is not presented since the corresponding feedback delay time ratios can be found in the region with $\tau_1 > \tau_2$ when the roles of the two

delays exchange. Obviously, the different delay times between the two feedback loops are good for the phase noise suppression. The phase noise can be reduced to as low as 0.0008. The result also indicates that some special ratios, such as 1/3, 1/2, 2/3 and 1 should be avoided, which are very similar to the case in DFB lasers [21].

4. Conclusion

In conclusion, characteristics of microwave photonic signal generation based on period-one dynamic of a VCSEL have been numerically investigated. In this study, the linewidth, phase noise, power and second harmonic ratio of the generated microwave photonic signal have been investigated in detail. The results show that the microwave signals with a wide range of microwave frequency have medium linewidth of ~5 MHz for the scheme with optical injection only. When single or double optical feedback is introduced to the VCSEL, the linewidth of the generated microwave is significantly reduced. When the feedback strengths in two feedback loops are set equally for double optical feedback, the effect of optical feedback on the linewidth reduction is not much different from that using single feedback with the same total feedback strengths. However, in terms of phase noise suppression, the double feedback performs better than single feedback because of side-peak suppression with double feedback. The effect of feedback delay time on the characteristic of the generated microwave indicates that longer delay time benefits the linewidth reduction. However, for single feedback, there is an optimized feedback delay time to obtain a minimum phase noise due to the competition of the external-cavity modes. For double feedback, the feedback ratio and delay time ratio between the two feedback loops can also impact the performance of the generated microwave. According to our results, the closer the feedback strengths from the two feedback loops, the lower the phase noise. For the selection of the feedback delay times in a double feedback configuration, some special feedback delay time ratios such as 1/3, 1/2, 2/3, 3/4 and 1 should be avoided to reduce the phase noise.

Funding. This work was supported in part by research projects of the DSP Centre funded by the European Regional Development Fund (ERDF) through the Welsh Government.

Acknowledgments. D. Chang thanks the support of Bangor University's Great Heritage PhD studentship. H. Lin thanks the support of Bates College Phillips Fellowship.

References

1. J. J. O'Reilly, P. M. Lane, R. Heidemann, and R. Hofstetter, "Optical generation of very narrow linewidth millimetre wave signals," *Electron. Lett*. **28**(25), 2309–2311 (1992).
2. O. Kjebon, R. Schatz, S. Lourdudoss, S. Nilsson, B. Stalnacke, and L. Backbom, "30 GHz direct modulation bandwidth in detuned loaded InGaAsP DBR lasers at 1.55 μm wavelength," *Electron. Lett.* **33**(6), 488–489 (1997).
3. S. Pan and J. Yao, "Wideband and frequency-tunable microwave generation using an optoelectronic oscillator incorporating a Fabry-Perot laser diode with external optical injection," *Opt. Lett.* **35**(11), 1911–1913 (2010).
4. Y. H. Hung and S. K. Hwang, "Photonic microwave amplification for radio-over-fiber links using period-one nonlinear dynamics of semiconductor lasers," *Opt. Lett.* **38**(17), 3355–3358 (2013).
5. F. Li and A. S. Helmy, "Gigahertz to terahertz tunable all-optical single-side-band microwave generation via semiconductor optical amplifier gain engineering," *Opt. Lett*. **38**(22), 4542–4545 (2013).
6. K. Balakier, M. J. Fice, F. van Dijk, G. Kervella, G. Carpintero, A. J. Seeds, and C. C. Renaud, "Optical injection locking of monolithically integrated photonic source for generation of high purity signals above 100 GHz," *Opt. Express,* **22**(24), 29404–29412 (2014).
7. S. C. Chan, S. K. Hwang, and J. M. Liu, "Period-one oscillation for photonic microwave transmission using an optically injected semiconductor laser," *Opt. Express*, **15**(22), 14921–14935 (2007).
8. C. Chih-Hao, L. Chrostowski, and C. J. Chang-Hasnain, "Injection locking of VCSELs," *IEEE J. Sel. Top. Quantum Electron.* **9**(5), 1386-1393 (2003).
9. T. B. Simpson, J. M. Liu, M. Almulla, N. G. Usechak, and V. Kovanis, "Linewidth sharpening via polarization-rotated feedback in optically injected semiconductor laser oscillators," *IEEE J. Sel. Top. Quantum Electron.* **19**(4), Art. no. 1500807 (2013).
10. T. B. Simpson, J. M. Liu, M. Almulla, N. G. Usechak, and V. Kovanis, "Limit-cycle dynamics with reduced sensitivity to perturbations," *Phys. Rev. Lett.* **112**(2), Art. no. 023901 (2014).

11. A. Hurtado, I. D. Henning, M. J. Adams, and L. F. Lester, "Generation of tunable millimeter-wave and THz signals with an optically injected quantum dot distributed feedback laser," *IEEE Photon. J.* **5**(4), Art. no. 5900107 (2013)
12. L. Fan, G. Xia, J. Chen, X. Tang, Q. Liang, and Z. Wu, "High-purity 60GHz band millimeter-wave generation based on optically injected semiconductor laser under subharmonic microwave modulation," *Opt. Express*. **24**(16), 18252–18265 (2016).
13. C. Wang, R. Raghunathan, K. Schires, S. C. Chan, L. F. Lester, and F. Grillot, "Optically injected InAs/GaAs quantum dot laser for tunable photonic microwave generation," *Opt. Lett.* **41** (6), 1153–1156 (2016).
14. R. Michalzik, Ed., VCSELs-fundamentals, technology and applications of vertical-cavity surface-emitting lasers (Springer series in optical sciences), **166**. Berlin, Germany: Springer, 2013, ch. 2.
15. A. Quirce, A. Valle, H. Lin, D. W. Pierce and Y. Zhang, "Photonic generation of high-frequency microwave signals utilizing a multi-transverse-mode vertical-cavity surface-emitting laser subject to two-frequency orthogonal optical injection," *J. Opt. Soc. Amer. B*. **29**(12), 3259–3269 (2012).
16. P. Perez, A. Quirce, A. Valle, A. Consoli, I. Noriega, L. Pesquera, I. Esquivias, "Photonic generation of microwave signals using a single mode VCSEL subject to double-beam orthogonal optical injection," *IEEE Photon. J*. **7**(1), Art. no. 5500614 (Feb. 2015).
17. H. Lin, S. Ourari, T. Huang, A. Jha, A. Briggs, and N. Bigagli, "Photonic microwave generation in multimode VCSELs subject to orthogonal optical injection," *J. Opt. Soc. Amer. B*. **34**(11), 2381–2389 (Nov. 2017).
18. S. Ji, Y. Hong, P. S. Spencer, J. Benedikt, and I. Davies, "Broad tunable photonic microwave generation based on period-one dynamics of optical injection vertical-cavity surface-emitting lasers," *Opt. Express*, **25**(17), 19863–19871 (Aug. 2017).
19. M. Pochet, T. Locke, and N. G. Usechak, "Generation and modulation of a millimeter-wave subcarrier on an optical frequency generated via optical injection," *IEEE Photon. J*. **4**(5), 1881–1891 (Oct. 2012).
20. C. H. Cheng, C. W. Lee, T. W. Lin, and F. Y. Lin, "Double-frequency laser Doppler velocimeter for speckle noise reduction and coherence enhancement," *Opt. Express*. **20**(18), 20255–20265 (2012).
21. J. P. Zhuang and S. C. Chan, "Phase noise characteristics of microwave signals generated by semiconductor laser dynamics," *Opt. Express*. **23**(3), 2777–2797 (Feb. 2015).
22. T. B. Simpson and F. Doft, "Double-locked laser diode for microwave photonics applications," *IEEE Photon. Technol. Lett.* **11**(11), 1476–1478 (Nov. 1999).
23. P. Zhou, F. Zhang, D. Zhang, and S. Pan, "Performance enhancement of an optically-injected-semiconductor laser-based optoelectronic oscillator by subharmonic microwave modulation," *Opt. Lett*. **43**(21), 5439–5442 (2018).
24. S. C. Chan and J. M. Liu, "Tunable narrow-linewidth photonic microwave generation using semiconductor laser dynamic," *IEEE J. Sel. Top. Quantum Electron*. **10**(5), 1025–1032 (2004)
25. H. Y. Pang, X. D. Lin, Z. M. Wu, T. Deng and G. Q. Xia, "Widely tunable narrow-linewidth photonic microwave generation using optically injected semiconductor laser combined with optoelectronic loops," Acta Photonica Sinica. **47**(1), Art. no. UNSP 0114003 (2018).
26. K.-H. Lo, S.-K. Hwang, and S. Donati, "Optical feedback stabilization of photonic microwave generation using period-one nonlinear dynamics of semiconductor lasers," *Opt. Express*. **22**(15), 18648–18661 (2014).
27. J. P. Zhuang and S. C. Chan, "Tunable photonic microwave generation using optically injected semiconductor laser dynamics with optical feedback stabilization," *Opt. Lett.* **38**(3), 344–346 (Feb. 2013).
28. C. Xue, S. Ji, Y. Hong, N. Jiang, H. Li, and K. Qiu, "Numerical investigation of photonic microwave generation in an optically injected semiconductor laser subject to filtered optical feedback," *Opt. Express*. **27**(4), 5065-5082 (2019).
29. B. Sun, J. G. Wu, S. Wang, Z. M. Wu, and G. Q. Xia, "Theoretical and experimental investigation on the narrow-linewidth photonic microwave generation based on parallel polarized optically injected 1550 nm vertical-cavity surface-emitting laser," *Acta Phys. Sinica*. **65**(1), Art. no. 014207 (2016).
30. Y.H. Hung and S.K. Hwang, "Photonic microwave stabilization for period-one nonlinear dynamics of semiconductor lasers using optical modulation sideband injection locking," *Optics Express*, **23**, 6520–6532 (2015)
31. S. Ji, C. Xue, A. Valle, P. S. Spencer, H. Li, and Y. Hong, "Stabilization of photonic microwave generation in vertical-cavity surface-emitting lasers with optical injection and feedback," *IEEE J. Lightw. Technol*. **36**(19), 4347-4353 (2018).
32. F. D. Coarer A. Quirce, P. Perez, A. Valle, L. Pesaquera, M. Sciamanna, H. Thienpont and K. Panajotov, "Injection locking and polarization switching bistability in a 1550 nm VCSEL subject to parallel optical injection," *IEEE J. Sel. Topics in Quantum Electron*. **23**(6), Art no. 1800910 (2017).
33. T. B. Simpson, J. M. Liu, M. AlMulla, N. G. Usechak, and V. Kovanis, "Limit-cycle dynamics with reduced sensitivity to perturbations," Phys. Rev. Lett., **112**, Art. no. 023901 (2014).
34. K. H. Lo, S. K. Hwang, and S. Donati, "Numerical study of ultrashort-optical- feedback-enhanced photonic microwave generation using optically injected semiconductor lasers at period-one nonlinear dynamics," Optics Express, **25**, 31595–31611 (2017).